Water vapor diffusion effects on gas dynamics in a sonoluminescing bubble

Ning Xu,[1] Robert E. Apfel,[1,*] Anthony Khong,[1] Xiwei Hu,[2] and Long Wang[3]
[1]*Department of Mechanical Engineering, Yale University, New Haven, Connecticut 06520, USA*
[2]*College of Electric and Electronic Engineering, Huazhong University of Science and Technology, Wuhan 430074, People's Republic of China*
[3]*Institute of Physics, Chinese Academy of Sciences, Beijing 100080, People's Republic of China*
(Received 3 December 2002; published 23 July 2003)

Calculations based on a consideration of gas diffusion of gas dynamics in a sonoluminescing bubble filled with a noble gas and water vapor are carried out. Xenon-, argon-, and helium-filled bubbles are studied. In the absence of shock waves, bubble temperatures are found to be decreased, a decrease attributable to the large heat capacity of water vapor. Peak bubble temperature reductions are seen in bubbles containing Xe or Ar but not in those containing He. Further extrapolations provide evidence for the occurrence of shock waves in bubbles with Xe and water vapor. No shock waves are observed in bubbles with Ar or He.

DOI: 10.1103/PhysRevE.68.016309 PACS number(s): 78.60.Mq, 51.20.+d, 52.35.Tc

Intense light emitted from a bubble levitated in a liquid driven by an ultrasound is known as a single-bubble sonoluminescence (SBSL) [1]. An intriguing property of SBSL is its high energy convergence [2]. A lot of theoretical work [3–8] has indicated that high temperatures can be generated in a sonoluminescing bubble, and hence light can be induced from the hot gases trapped in the bubble. Among the theories that have been proposed to account for the mechanism of the high energy convergence, that relating to heat-induced SBSL has been most invoked. How to boost SBSL and apply SBSL's high energy convergence remain areas of immense interest. A method recently proposed by Apfel to boost sonoluminescence involves decreasing the ultrasound frequency. This proposal was theoretically ''realized'' by Hilgenfeldt and Lohse [9]. However, experiments did not obtain the predicted results. It was shown that the SBSL intensity at lower ultrasound frequency was not increased. Recent theoretical work attributed this inconsistency between the theory and the experiment to the presence of water vapor in the bubble: the large heat capacity of water vapor might decrease the temperatures in the bubble. The presence of water vapor was not considered in earlier theoretical calculations.

Some recent studies carried out to study the effects of water vapor include the work of Moss *et al.* [10]. The SBSL intensity was found to be sensitive to the quantity of water vapor in the bubble. Storey and Szeri included some primary chemical reactions involving water in their model and concluded that the presence of water vapor significantly decreased the temperatures in the bubble [11].

In previous theoretical work, the possibility of shock wave occurrence in a sonoluminescing bubble was noted. In disregarding neutral gas thermal conduction and viscosity in their calculations, Wu and Roberts [3] and Moss *et al.* [4,5] showed that strong shock waves could occur. However, Vuong and Szeri [6] and Yuan *et al.* [8] presented contrary results that no shock wave occurrence could be observed in noble gas bubbles as neutral gas thermal conduction and viscosity were considered. Yuan *et al.* [8] also found that using the Keller equation instead of the Rayleigh-Plesset equation to describe the motion of the bubble wall reduced the occurrence of shock waves because of the effect of water compressibility. The presence of water vapor in the bubble was largely ignored in these studies. Although Moss *et al.* considered the water vapor's influence on the gas dynamics in the bubble [10], the neutral gas thermal conduction and viscosity and the possibility of gas diffusion which should occur in a gas mixture were not considered.

Some calculations showed that gas diffusion could have significant effects on the gas dynamics. Diffusion can be driven by the spatial gradient of the species concentration, temperature, and pressure. Previous calculations showed that gradients of these physical quantities existed in a sonoluminescing bubble, especially during the final stage of the bubble collapse. If shock waves could occur, the gradients would even be steeper. Xu *et al.* considered the plasma diffusion in their model and found that a very strong electric field could be generated in a sonoluminescing bubble due to charge separation [12]. Storey and Szeri carried out a calculation of the gas diffusion in a bubble filled with argon and helium [13]. These studies indicate that gas diffusion may have significant influences on the gas dynamics in a sonoluminescing bubble and hence may need to be considered if water vapor is present.

Assuming, as in previous calculations, spherical symmetry of the bubbles, we can simplify the problems to one-dimensional cases. The motion of the bubble wall can thus be described by the Rayleigh-Plesset (RP) equation. The earlier type of the RP equation was derived based on the assumption of the incompressibility of the liquid around the bubble. This approximation is valid except for the final stage of the bubble collapse. During the bubble's final collapse, the Mach number of the bubble wall is so large that the approximation of liquid incompressibility may introduce large errors. Yuan *et al.* [8] compared the influences of the different types of the RP equation on the gas dynamics and showed that the inclusion of liquid compressibility in the equation weakened the disturbances of the gas in the bubble. In this paper, we report our studies of bubbles containing a noble

*Deceased.

gas and some amount of water vapor. The modified Keller equation is employed as the equation for the bubble wall:

$$(1-M)R\ddot{R}+\frac{3}{2}\left(1-\frac{M}{3}\right)\dot{R}^2 = (1+M)\left[H_b-\frac{1}{\rho_{lb}}P_a\left(t+\frac{R}{c_{lb}}\right)\right]+\frac{R}{c_{lb}}\frac{dH_b}{dt}, \quad (1)$$

where R, H_b, ρ_{lb}, and c_{lb} are the bubble radius, enthalpy of the water at the bubble wall, density of the water at the bubble wall, and speed of sound in the water at the bubble wall, respectively. $M=\dot{R}/c_{lb}$ is the Mach number of the bubble wall, and $P_a(t)=-P_a'\sin(\omega_a t)$ is the pressure of the ultrasound applied to the bubble wall, where P_a' and ω_a are the amplitude and frequency of the ultrasound. The overdots are the derivatives with respect to time t.

The modified Tait form equation of state is applied to the water:

$$\frac{P_l+B}{P_{l\infty}+B}=\left(\frac{\rho_l}{\rho_{l\infty}}\right)^n, \quad (2)$$

where P_l, $P_{l\infty}$, ρ_l, and $\rho_{l\infty}$ are the pressure, ambient pressure, density, and ambient density of the water, respectively, $B=3049.13$ bars and $n=7.15$. At the bubble wall, the speed of sound c_{lb} and the enthalpy of the water H_b can thus be expressed as

$$c_{lb}=\sqrt{\frac{n(P_{lb}+B)}{\rho_{lb}}}, \quad (3)$$

$$H_b=\frac{n}{n-1}\left(\frac{P_{lb}+B}{\rho_{lb}}-\frac{P_{l\infty}+B}{\rho_{l\infty}}\right). \quad (4)$$

The pressure in the liquid at the bubble wall, P_{lb}, matches with the pressure of the gas on the other side of the bubble wall, $P(R,t)$, by

$$P_{lb}=P(R,t)+\tau_{rr}(R,t)-\frac{2\sigma}{R}-\frac{4\nu\rho_{lb}\dot{R}}{R}, \quad (5)$$

where τ_{rr}, σ, and ν are the normal components of the gas viscous stress, surface tension of the water, and kinetic viscosity of the water, respectively.

In order to describe the details of the gas dynamics in the bubble, the hydrodynamic equations are applied. Two models can be used to describe the diffusion processes. One is the multifluid model which applies the conservative equations to different species in a mixture separately and couples the species using some collision assumptions. However, it is hard to describe the transport coefficients of a species in the mixture. Hence, we use the other model, the diffusion model, which was also used in Ref. [13], to construct our calculations. Some water vapor is introduced in the bubble filled with a noble gas. Previous calculations showed that the bubble underwent expansion and collapse prior to light emission. Since the spatial distribution of the physical quantities in the bubble shown in previous calculations was nearly uniform during the bubble expansion and the early stage of the bubble collapse, we, therefore, only consider the diffusion processes at the start of the bubble collapse. The mass diffusion of the water vapor between the bubble and the surrounding water is not considered. This is somewhat reasonable. Before the final violent collapse of the bubble wall, even though the mass diffusion occurs at the interface, there is enough time for the gases to diffuse and maintain the nearly uniform spatial distributions of all the physical quantities. During the final collapse of the bubble wall, the collapse is too fast to let significant mass diffusion occur. The mass diffusion should be included and carefully studied if the exact amount of water vapor trapped in the bubble is to be known. However, the mass diffusion will not significantly change our qualitative analysis of the effects of diffusion on the gas dynamics in a sonoluminescing bubble. The species' temperatures are not separated, since it is known that different species collide frequently and reach uniform temperatures in a very short time. The gas dissociation, ionization, and some possible chemical reactions are not included in our model.

The mass, momentum, and energy conservative equations of the gas mixture in spherical coordinates are

$$\frac{D\rho}{Dt}+\frac{\rho}{r^2}\frac{\partial}{\partial r}(r^2u)=0, \quad (6)$$

$$\rho\frac{Du}{Dt}=-\frac{\partial}{\partial r}(P+\tau_{rr})-\frac{3\tau_{rr}}{r}, \quad (7)$$

$$\rho\frac{D}{Dt}\left(e+\frac{1}{2}u^2\right)=-\frac{1}{r^2}\frac{\partial}{\partial r}\{r^2[(P+\tau_{rr})u+q]\}, \quad (8)$$

where ρ, u, P, τ_{rr}, e, and q are, respectively, the density, velocity, pressure, normal stress tensor, internal energy, and heat flux of the gas mixture, r is the radial coordinate, and $D/Dt=\partial/\partial t+u\partial/\partial r$. Equation (7) is derived based on the relations that $\tau_{rr}=-2\tau_{\theta\theta}=-2\tau_{\phi\phi}$ in spherical coordinates.

The two species in the mixture satisfy the following relations:

$$\rho=\rho_1+\rho_2, \quad (9)$$

$$J_1=-J_2, \quad (10)$$

where ρ_i and $J_i=\rho_i U_i$ $(i=1,2)$ are the density and diffusion flux of the ith species, respectively, and $U_i=u_i-u$ $(i=1,2)$ is the diffusion velocity of the ith species, where u_i is the velocity of the ith species. Hence, to study the diffusion processes, we only need to calculate the diffusion of one species and derive that for the other using Eqs. (9) and (10). The diffusion of species 1 can be expressed by the following mass conservative equation:

$$\frac{D\rho_1}{Dt}+\frac{\rho_1}{r^2}\frac{\partial}{\partial r}(r^2u)=-\frac{1}{r^2}\frac{\partial}{\partial r}(r^2J_1). \quad (11)$$

The diffusion flux J_1 is assumed to be generated by the gradients of the mole fraction of species 1, y_1, temperature T, and pressure P, and hence satisfies

$$J_1 = -\frac{n^2 M_1 M_2}{\rho} D_{12}\left[\frac{\partial y_1}{\partial r} + \left(y_1 - \frac{\rho_1}{\rho}\right)\frac{\partial lnP}{\partial r} + k_T \frac{\partial lnT}{\partial r}\right], \tag{12}$$

where n is the number density of the mixture, M_i $(i=1,2)$ is the molecular weight of the ith species, D_{12} is the binary diffusion coefficient, and k_T is the thermal diffusion ratio.

The normal stress tensor and the heat flux of the gas mixture can be expressed as

$$\tau_{rr} = -\frac{4}{3}\mu\left(\frac{\partial u}{\partial r} - \frac{u}{r}\right), \tag{13}$$

$$q = -\lambda \frac{\partial T}{\partial r} + (h_1 - h_2) J_1, \tag{14}$$

where μ and λ are the viscosity and thermal conductivity of the gas mixture, respectively, and h_i $(i=1,2)$ is the enthalpy of the ith species.

Four transport coefficients, D_{12}, k_T, μ, and λ, are to be defined. Because the gases in a sonoluminescing bubble during the final collapse are under extreme conditions, it is hard to describe these coefficients exactly. Like Storey and Szeri [13], we employ the results derived from molecular theory, paying special attention to the corrections due to high pressures and the polarity of water vapor.

The viscosity of the gas mixture at low pressure can be approximately expressed as [14]

$$\mu = \mu^0 = \frac{y_1 \mu_1}{y_1 \phi_{11} + y_2 \phi_{12}} + \frac{y_2 \mu_2}{y_1 \phi_{21} + y_2 \phi_{22}}, \tag{15}$$

where μ_i $(i=1,2)$ in micropoise is the viscosity of the pure gas of the ith species, and the ϕ's are the parameters which are calculated from the Brokaw approximation [14]. The corrected expression due to high pressure is [14]

$$\mu = \mu^0 + \frac{1.08}{\xi}\left[e^{1.439\rho_r} - e^{-1.11\rho_r^{1.858}}\right] \ \mu\mathrm{P}, \tag{16}$$

where $\rho_r = \rho/\rho_c$ is the pseudoreduced mixture density and ξ is defined as $T_c^{1/6}/M^{1/2}P_c^{2/3}$, where P_c, ρ_c, and T_c are the pseudocritical pressure, density, and temperature of the mixture, respectively, and are calculated by modified Prausnitz and Gunn rules [14], and M is the mole fraction averaged molecular weight of the mixture. The thermal conductivity of the gas mixture at low pressure is approximately [14]

$$\lambda = \lambda^0 = \frac{y_1 \lambda_1}{y_1 A_{11} + y_2 A_{12}} + \frac{y_2 \lambda_2}{y_1 A_{21} + y_2 A_{22}}, \tag{17}$$

where λ_i $(i=1,2)$ in cal/cm s K is the thermal conductivity of the ith species, and the A's are the parameters which are calculated from the formulas in Ref. [14]. The high pressure correction of the thermal conductivity of the mixture is [14]

$$\lambda = \lambda^0 + \frac{1.40\times 10^{-7}}{\Gamma Z_c^5}(e^{0.535\rho_r} - 1) \ \text{cal/cm s K}, \quad \rho_r < 0.5,$$

$$\lambda = \lambda^0 + \frac{1.31\times 10^{-7}}{\Gamma Z_c^5}(e^{0.67\rho_r} - 1.069) \ \text{cal/cm s K}, \quad 0.5 < \rho_r < 2.0, \tag{18}$$

$$\lambda = \lambda^0 + \frac{2.976\times 10^{-8}}{\Gamma Z_c^5}(e^{1.155\rho_r} + 2.016) \ \text{cal/cm s K}, \quad \rho_r > 2.0,$$

where $Z_c = P_c/\rho_c \bar{R} T_c$ and $\Gamma = T_c^{1/6} M^{1/2}/P_c^{2/3}$ are functions of the pseudocritical parameters, and $\bar{R}$ is the gas constant. The thermal diffusion ratio can be expressed as [15]

$$k_T = \frac{y_1 y_2}{6\lambda}\frac{S^{(1)} y_1 - S^{(2)} y_2}{X_\lambda + Y_\lambda}(6C_{12}^* - 5), \tag{19}$$

where $S^{(1)}$, $S^{(2)}$, X_λ, Y_λ, and C_{12}^* are functions defined in Ref. [15]. The diffusion coefficient adopted here is [14]

$$D_{12} = 1.858\times 10^{-3} T^{3/2}\frac{[(M_1+M_2)/M_1 M_2]^{1/2}}{P\sigma_{12}^2 \Omega_D} \ \text{cm}^2/\text{s}, \tag{20}$$

where $\sigma_{12} = (\sigma_1 \sigma_2)^{1/2}$ in angstrom is the characteristic length, σ_i $(i=1,2)$ is the molecular diameter of the ith species, and Ω_D is the diffusion collision integral.

The equation of state is also required to solve the system. Here, we use the van der Waals form of the equation of state, which is commonly used in SBSL simulations as a good approximation when dissociation and ionization of gases are not considered,

$$P = \frac{nkT}{1 - b\rho}, \tag{21}$$

$$e = \frac{kT}{\rho}\left(\frac{n_1}{\gamma_1 - 1} + \frac{n_2}{\gamma_2 - 1}\right), \tag{22}$$

where k is the Boltzmann constant, b is the excluded volume of the gas mixture, and n_i and γ_i $(i=1,2)$ are the number density and specific heat ratio of the ith species.

As proposed by Vuong and Szeri [6], a heat flux exists across the bubble wall due to the temperature gradients. The temperature in the water can be described by the energy conservative equation

$$\frac{DT_l}{Dt} = \frac{\lambda_l}{\rho_l c_{Pl} r^2}\frac{\partial}{\partial r}\left(r^2 \frac{\partial T_l}{\partial r}\right), \tag{23}$$

where T_l, λ_l, and c_{Pl} are the temperature, thermal conductivity, and specific heat at constant pressure of the water, respectively. We use the same technique as that used in Ref. [6] to manipulate this equation. Equation (23) can then be rewritten as

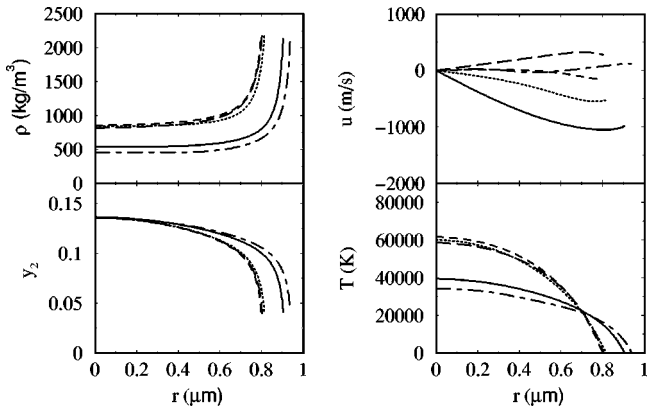

FIG. 1. The spatial profiles of the density ρ, velocity u, mole fraction of water vapor y_2, and temperature T in a bubble filled with 90% Xe and 10% water vapor. The temporal sequence of the five curves is t_1 (solid line), $<t_2$ (dotted line), $<t_3$ (dashed line), $<t_4$ (long dashed line), $<t_5$ (dot-dashed line). No shock waves are observed.

$$\frac{DT_l}{Dt}=\frac{\lambda_l}{\rho_l c_{Pl}}\frac{\partial}{\partial\sigma}\left[(3\sigma+R^3)^{4/3}\frac{\partial T_l}{\partial\sigma}\right], \tag{24}$$

which introduces a Lagrangian coordinate $\sigma=(r^3-R^3)/3$. At the bubble wall, the continuity of the heat flux leads to

$$\lambda\frac{\partial T}{\partial r}\bigg|_{r=R}=\lambda_l\frac{\partial T_l}{\partial r}\bigg|_{r=R}, \tag{25}$$

which is a physical boundary condition applied to the bubble wall.

We employ the second-order MacCormack scheme to solve Eqs. (6), (7), (8), and (11) numerically. An implicit central finite difference method is applied to Eq. (24) in order to stabilize the calculations. The bubble interior is divided into 400 grids and 200 points are applied to the surrounding water.

The following parameters are chosen in our calculations: $P_a'=1.35$ atm, $\omega_a=2\pi\times 26.5$ kHz, $R_0=4.5$ μm, $P_{l\infty}=1$ atm, $T_0=300$ K, $\rho_{l\infty}=996.6$ kg/m^3, $\sigma=0.0725$ N/m, $\nu=0.857\times10^{-6}$ m^2 s^{-1}, $\lambda_l=0.609$ W m^{-1} K^{-1}, and $c_{Pl}=4179$ J kg^{-1} K^{-1}. The noble gases studied are He, Ar, and Xe. In a gas mixture, the heavier gas tends to move to the cooler region due to diffusion. Intuitively, we can imagine that diffusion may be more significant in a gas mixture filled with gases with larger differences in molecular weights. Therefore, the Xe and He bubbles should exhibit stronger diffusion behavior and should be representative models of the question about gas diffusion in SBSL.

The water vapor concentration is varied in order to observe the influence of the amount of the water vapor on the gas dynamics. Figure 1 shows five snapshots of the spatial profiles of the density, velocity, temperature of the mixture, and the mole fraction of water vapor in a bubble filled with 90% (mole fraction) Xe and 10% water vapor during the bubble's final collapse and the first rebound. No shock waves are produced. Only some wavy disturbances propagate such as those described in Refs. [6,8]. The water vapor accumulates at the bubble center as the waves propagate inwards, which can be seen more clearly in Fig. 2(a). This is consistent with the diffusion, because Xe has a larger molecular weight than water vapor and the bubble center is hotter than that at the periphery. Since no shock waves occur, the gases are compressed quasiadiabatically. Water vapor has smaller specific heat ratio compared to noble gases. The presence of water vapor thus decreases the temperatures. In Fig. 2(b), the temperatures at the bubble center for three cases are compared: pure Xe, a mixture of Xe and water vapor without diffusion, and a mixture with diffusion. The temperature in the pure Xe bubble is the highest. Diffusion leads to the lowest temperature among these three cases, because more water vapor congregates at the bubble center. The presence of water vapor can significantly decrease the temperatures, as shown in Fig. 2(b), which can explain the failure of the method to boost SBSL by decreasing the driving frequency. If the driving frequency is decreased, the time for bubble expansion is now longer. More water vapor can diffuse into the bubble, which can greatly decrease the high temperatures that can be achieved in a pure noble gas bubble. For noble gases with larger molecular weights than water vapor, even more water vapor enters the hot regions due to diffusion and therefore decreases the temperatures further. According to the assumption of heat-induced SBSL, any increase in light intensity cannot be achieved.

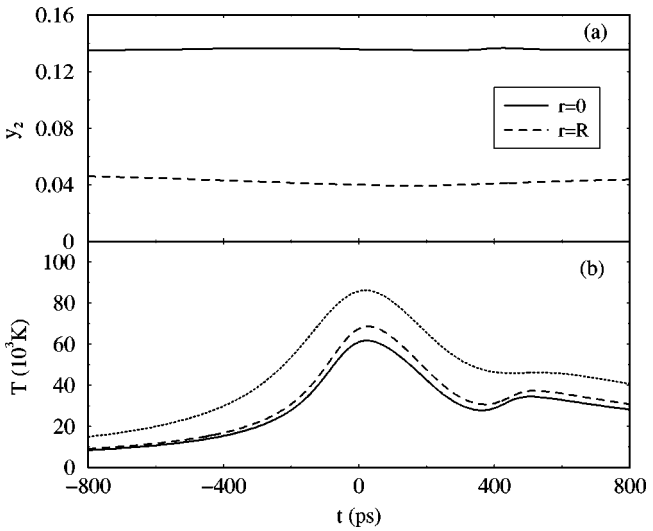

FIG. 2. The time evolutions of (a) mole fraction of water vapor at the center ($r=0$) and wall ($r=R$) of a bubble filled with 90% Xe and 10% water vapor and (b) temperatures at the bubble center for three cases: a bubble filled with pure Xe (dotted line), a bubble filled with 90% Xe and 10% water vapor without diffusion (dashed line), and a bubble filled with 90% Xe and 10% water vapor with diffusion (solid line).

Previous calculations [10] showed that the presence of water vapor in a gas bubble could promote the occurrence of shock waves due to water vapor's low specific heat ratio. The mole fraction of the water vapor is thus increased to test if shock waves can occur in our models. Figure 3 shows the spatial profiles of the density, velocity, and temperature of the gas mixture, and the mole fraction of the water vapor in a bubble filled with 70% (mole fraction) Xe and 30% water

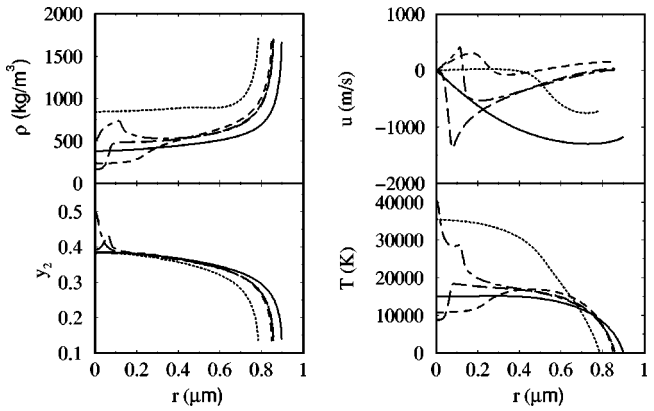

FIG. 3. The spatial profiles of the density ρ, velocity u, mole fraction of water vapor y_2, and temperature T in a bubble filled with 70% Xe and 30% water vapor. The temporal sequence of the five curves is t_1 (solid line), $<t_2$ (dotted line), $<t_3$ (dashed line), $<t_4$ (long dashed line), $<t_5$ (dot-dashed line). Shock waves are observed.

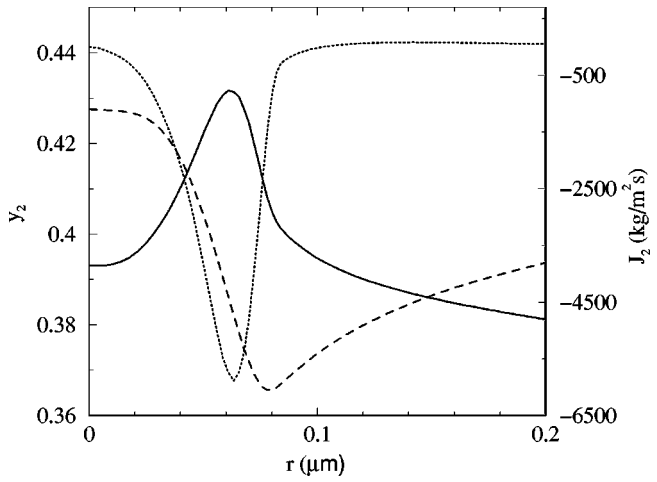

FIG. 5. The spatial profiles of the mole fraction y_2 (solid line) and mass flux J_2 (dotted line) at the shock front. The dashed line is the profile of the velocity of the shock wave. All the parameters are the same as those in Figs. 3 and 4.

vapor. During the initial collapse of the bubble, the inward disturbance is much stronger than that in Fig. 1 and develops into a weak shock wave as it propagates towards the bubble center. The shock wave becomes more obvious after it is reflected from the bubble wall and becomes stronger as it propagates towards the bubble center again. From Fig. 4(b) we can see that a peak temperature up to nearly 110 000 K, which is much higher than the highest temperature we obtain in the pure Xe bubble [see Fig. 2(b)], is achieved when the shock wave is reflected from the bubble center. This temperature peak has a narrower time width. The mole fraction of the water vapor at the bubble center also undergoes an abrupt surge due to the shock wave's reflection, which is shown in Fig. 4(a).

In Fig. 5, we plot the mole fraction and diffusion flux of water vapor across the shock front. The lighter gas is more easily propelled in front of the wave front. Hence, in the mixture of Xe and water vapor, the diffusion flux of water vapor is in the same direction of the wave propagation. At the shock front, the diffusion flux of water vapor reaches a peak which leads to the congregation of water vapor here. A peak water vapor concentration is thus produced at the shock front. Since water vapor has a lower specific heat ratio compared to the noble gases, the congregation of water vapor dramatically decreases the speed of sound at the shock front. The decrease of the speed of sound increases the Mach number of the wave. The shock wave is thus strengthened. The congregation of water vapor and the development of shock wave promote each other during the propagation of the shock wave. This can be seen from Fig. 3. As the shock wave hits the origin of the bubble, the strength of the shock wave and the water vapor fraction both reach their maxima.

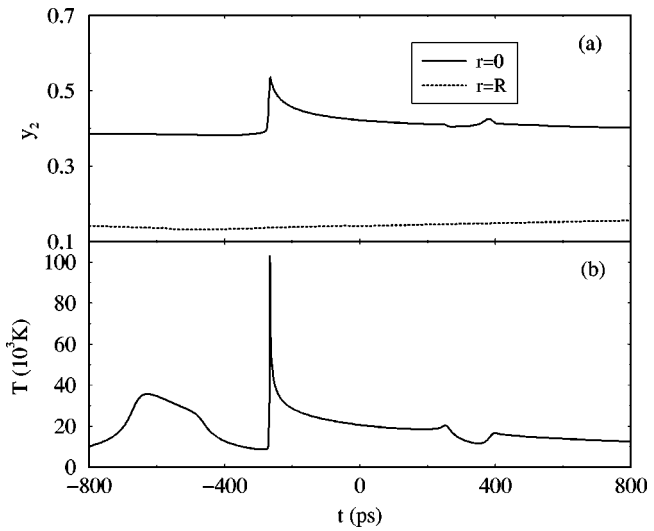

FIG. 4. The time evolutions of (a) mole fraction of water vapor at the center ($r=0$) and wall ($r=R$) of the bubble and (b) temperature at the bubble center. The bubble is the same as that in Fig. 3.

Similar calculations for a bubble filled with 70% (mole fraction) Ar and 30% water vapor are carried out. No shock wave is found in this case. Because the difference in the molecular weight between Ar and water vapor is not so large as that between Xe and water vapor, the congregation of water vapor at the bubble center is not remarkable. The maximum mole fraction of water vapor at the bubble center is only about 33%, as shown in Fig. 6(a). This means that the diffusion in this bubble is not strong and can be neglected. The inclusion of water vapor cools the bubble. Since the diffusion is weak, the temperatures at the bubble center with and without diffusion are only slightly different, as shown in Fig. 6(b). Although no shock waves are observed in this case, their absence in an Ar bubble undergoing SBSL cannot yet be ruled out.

Unlike Xe and Ar, He has a smaller molecular weight than water vapor. The water vapor diffusion in a He bubble is, therefore, predictably different from that in the Xe and Ar bubbles. In Fig. 7, we plot five snapshots of the spatial profiles of the density, velocity, and temperature of the gas mixture, and the mole fraction of water vapor in a bubble filled with 70% (mole fraction) He and 30% water vapor during

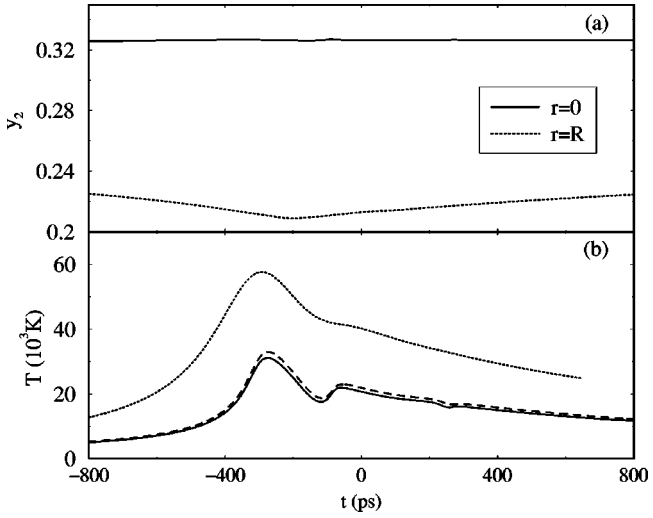

FIG. 6. The time evolutions of (a) mole fraction of water vapor at the center ($r=0$) and wall ($r=R$) of a bubble filled with 70% Ar and 30% water vapor and (b) temperatures at the bubble center for three cases: a bubble filled with pure Ar (dotted line), a bubble filled with 70% Ar and 30% water vapor without diffusion (dashed line), and a bubble filled with 70% Ar and 30% water vapor with diffusion (solid line).

the bubble's final collapse and the first rebound. Unlike in Fig. 1, the mole fractions of water vapor have positive gradients. There exists a tendency for the water vapor to congregate at the periphery of the bubble, because the molecular weight of water vapor is much larger than that of He and the temperatures in the bubble have negative gradients. It is hard to generate shock waves in a pure He bubble due to the small molecular weight of He. Although the presence of water vapor can help lower the speed of sound, unlike what is observed in the bubbles filled with Xe, the diffusion process decreases the concentration of water vapor just ahead of the wave front (the direction of the flux of water vapor is opposite to the direction of wave propagation) and reduces the

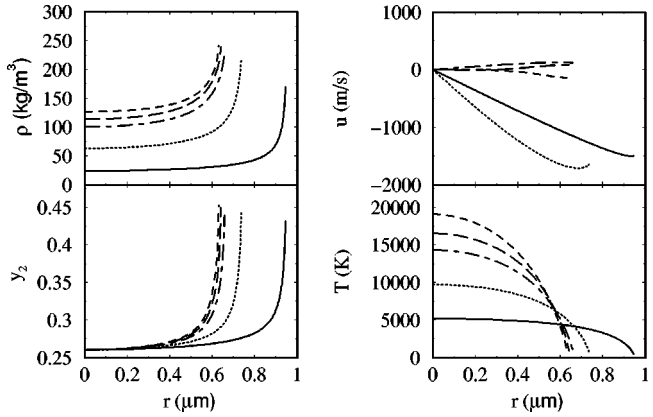

FIG. 7. The spatial profiles of the density ρ, velocity u, mole fraction of water vapor y_2, and temperature T in a bubble filled with 70% He and 30% water vapor. The temporal sequence of the five number marked curves is t_1 (solid line), $<t_2$ (dotted line), $<t_3$ (dashed line), $<t_4$ (long dashed line), $<t_5$ (dot-dashed line). No Shock waves are observed.

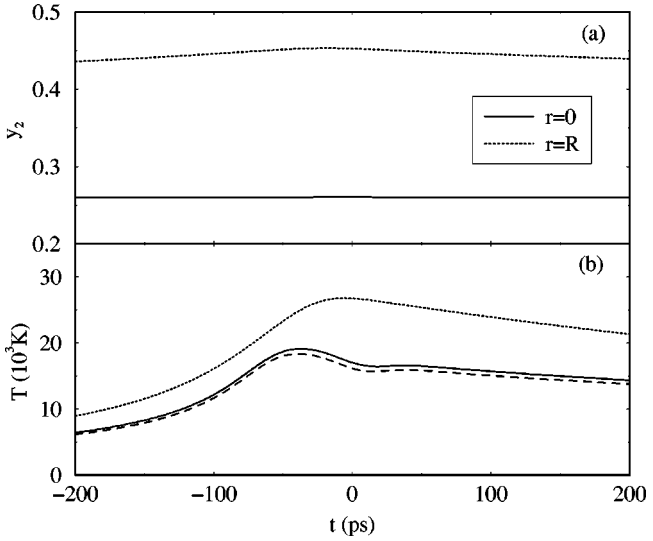

FIG. 8. The time evolutions of (a) mole fraction of water vapor at the center ($r=0$) and wall ($r=R$) of a bubble filled with 70% He and 30% water vapor and (b) temperatures at the bubble center for three cases: a bubble filled with pure He (dotted line), a bubble filled with 70% He and 30% water vapor without diffusion (dashed line), and a bubble filled with 70% He and 30% water vapor with diffusion (solid line).

possibility of shock wave occurrence. As can be seen, there are only some wavy disturbances in the bubble. In Fig. 8(a), we plot the mole fraction of water vapor at the bubble center and the bubble wall. In contrast to those shown in the Xe and Ar cases, the water vapor concentration at the bubble wall is higher than that at the bubble center. Figure 8(b) compares the temperatures at the bubble center of three cases: pure He, a mixture of He and water vapor with diffusion, and a mixture without diffusion. It is still the case that the inclusion of water vapor lowers the temperatures in the absence of shock waves. However, diffusion reduces the concentration of water vapor at the bubble center. The temperatures in bubbles with diffusion are thus higher than those without diffusion.

Calculations of gas dynamics in bubbles filled with a noble gas and water vapor, with a focus on gas diffusion, are carried out. The following conclusions can be drawn from the results of the calculations: (i) the presence of water vapor decreases the peak temperatures in a noble gas bubble due to the large heat capacity of water vapor if only weak compressional waves propagate; (ii) in the Ar and Xe bubbles, water vapor tends to congregate around the bubble center during the bubble's final collapse, while in a He bubble, water vapor tends to diffuse to the outer layers of the bubble; (iii) water vapor helps to strengthen the disturbances in the bubble due to its low specific heat ratio; (iv) water vapor diffusion in the Xe and Ar bubbles can enhance the disturbances further due to water vapor's congregation in front of the wave front, while in a He bubble it weakens the disturbances because of the reversed diffusion behavior; (v) shock waves are observed in a bubble filled with 70% Xe and 30% water vapor; (vi) in the absence of shock waves, water vapor diffusion decreases the peak temperatures in the Xe and Ar bubbles, while increasing the peak temperatures in a He bubble.

The conclusion that no shock waves can occur in a noble gas bubble made from previous calculations [6,8] is not comprehensive. The inclusion of water vapor and the diffusion process increases the possibility of shock wave occurrence, as was also noted in Ref. [11]. Transient high temperatures can be induced by the compression of shock waves. We do not include the light emission mechanisms in our present calculations, but we can predict that these high temperatures will not significantly influence the SBSL spectra, because they occur over a very short time and only exist in the thin layers around the bubble center, as shown in our calculations. Hence, water vapor and its diffusion are important in determining the gas dynamics in a SBSL bubble, and may provide us a better understanding of SBSL.

This work was partly supported by DARPA (Grant No. N00014-99-1-0793) and NASA (Grant No. NAG3-2377).

[1] F. Gaitan and L.A. Crum, J. Acoust. Soc. Am. **87**, S141 (1990).
[2] B.P. Barber and S.J. Putterman, Nature (London) **352**, 318 (1991).
[3] C.C. Wu and P.H. Roberts, Phys. Rev. Lett. **70**, 3424 (1993).
[4] W.C. Moss *et al.*, Phys. Fluids **6**, 2979 (1994).
[5] W.C. Moss, D.B. Clarke, and D.A. Young, Science **276**, 1398 (1997).
[6] V.Q. Vuong and A.J. Szeri, Phys. Fluids **8**, 2354 (1996).
[7] N. Xu, L. Wang, and X. Hu, Phys. Rev. E **57**, 1615 (1998).
[8] L. Yuan *et al.*, Phys. Rev. E **57**, 4265 (1998).
[9] S. Hilgenfeldt and D. Lohse, Phys. Rev. Lett. **82**, 1036 (1999).
[10] W.C. Moss *et al.*, Phys. Rev. E **59**, 2986 (1999).
[11] B.D. Storey and A.J. Szeri, Proc. R. Soc. London, Ser. A **456**, 1685 (2000).
[12] N. Xu, L. Wang, and X. Hu, Phys. Rev. Lett. **83**, 2441 (1999).
[13] B.D. Storey and A.J. Szeri, J. Fluid Mech. **396**, 203 (1999).
[14] R.C. Reid, J.M. Prausnitz, and T.K. Sherwood, *The Properties of Gases and Liquids*, 3rd ed. (McGraw-Hill, New York, 1977).
[15] J.O. Hirschfelder, C.F. Curtiss, and R.B. Bird, *Molecular Theory of Gases and Liquids* (Wiley, New York, 1964).